Balanced Central Schemes for the Shallow Water Equations on Unstructured Grids

Steve Bryson[*]   Doron Levy[†]

March 23, 2004

Abstract

We present a two-dimensional, well-balanced, central-upwind scheme for approximating solutions of the shallow water equations in the presence of a stationary bottom topography on triangular meshes.

Our starting point is the recent central scheme of Kurganov and Petrova (KP) for approximating solutions of conservation laws on triangular meshes. In order to extend this scheme from systems of conservation laws to systems of balance laws one has to find an appropriate discretization of the source terms. We first show that for general triangulations there is no discretization of the source terms that corresponds to a well-balanced form of the KP scheme. We then derive a new variant of a central scheme that can be balanced on triangular meshes.

We note in passing that it is straightforward to extend the KP scheme to general unstructured conformal meshes. This extension allows us to recover our previous well-balanced scheme on Cartesian grids. We conclude with several simulations, verifying the second-order accuracy of our scheme as well as its well-balanced properties.

Key words. Shallow water equations, central schemes, balance laws, unstructured grids.

AMS(MOS) subject classification. Primary 65M06; secondary 76B15.

1 Introduction

We consider a flow in a two-dimensional channel with a bottom elevation given by $B(\vec{x})$, where $\vec{x} = (x, y)$. Let $H(\vec{x}, t)$ represent the fluid depth above the bottom, and $\vec{u}(\vec{x}, t) = (u(\vec{x}, t), v(\vec{x}, t))$ be the fluid velocity. The top surface at any time t is denoted by $w(\vec{x}, t) = B(\vec{x}) + H(\vec{x}, t)$.

The shallow water equations, introduced by Saint-Venant in [22], are commonly used to model flows in rivers or coastal areas. When written in terms of the top surface w and the momentum

[*]Program in Scientific Computing/Computational Mathematics, Stanford University and the NASA Advanced Supercomputing Division, NASA Ames Research Center, Moffett Field, CA 94035-1000; bryson@nas.nasa.gov

[†]Department of Mathematics, Stanford University, Stanford, CA 94305-2125; dlevy@math.stanford.edu

(Hu, Hv) these equations are of the form

$$\begin{cases} w_t + (Hu)_x + (Hv)_y = 0, \\[2mm] (Hu)_t + \left[\dfrac{(Hu)^2}{w - B} + \dfrac{1}{2}(w - B)^2 \right]_x + \left[\dfrac{(Hu)(Hv)}{w - B} \right]_y = -g(w - B)B_x, \\[3mm] (Hv)_t + \left[\dfrac{(Hu)(Hv)}{w - B} \right]_x + \left[\dfrac{(Hv)^2}{w - B} + \dfrac{1}{2}(w - B)^2 \right]_y = -g(w - B)B_y. \end{cases} \qquad (1.1)$$

This choice of variables is particularly suitable for dealing with stationary steady-state solutions (see [12, 21] for details). For simplicity we fix the gravitational constant, g, from now on to be $g = 1$.

In this work we are interested in approximating solutions of (1.1) on triangular meshes. Our goal is to investigate how to adapt the semi-discrete central schemes on triangular meshes that were recently introduced by Kurganov and Petrova in [14] to this problem. We are interested in deriving a discretization of the source terms in (1.1) that preserves stationary steady-state solutions, as such solutions play an important role in the dynamics of (1.1).

Central schemes for conservation laws have become popular in recent years as a tool for approximating solutions for multi-dimensional systems of hyperbolic conservation laws. Like other Godunov-type schemes, central schemes are based on a three-step procedure: *a reconstruction step* in which an interpolant is reconstructed from previously computed cell-averages; *an evolution step* in which this interpolant is evolved exactly in time according to the equations; and *a projection step* in which the solution is projected back to cell-averages. When compared with other methods, central schemes are particularly appealing since they do not require any Riemann solvers and systems can be solved component-wise.

A first-order prototype of central schemes is the Lax-Friedrichs scheme [6]. A second-order extension is due to Nessyahu and Tadmor [19]. Extensions to two dimensions are due to Arminjon, Jiang and Tadmor [1, 11]. By estimating bounds on the local speeds of propagation of information from discontinuities, it is possible to pass to the semi-discrete limit (see [13, 15] and the references therein). There are several extensions of central schemes to unstructured grids. A fully discrete method is due to Arminjon *et al.* [2]; a recent semi-discrete scheme was proposed by Kurganov and Petrova in [14]. Balanced Central schemes for shallow water equations on Cartesian grids are due to Russo in the fully-discrete framework [21] (see also [18]) and to Kurganov and Levy in the semi-discrete framework [12].

There are many approaches to approximating solutions of (1.1). We refer, e.g. to [3, 4, 5, 7, 9, 16, 17, 20] and the references therein. Our goal in this paper is to show that balancing is also possible with central schemes. We would like to emphasize that this is the first time in which the balancing issues are treated for central schemes on unstructured grids.

The paper is organized as follows. We start in Section 2 with a brief overview of the KP central scheme on triangular meshes. We note that this scheme is not limited to triangular meshes and it can be equally well applied to general unstructured grids. We also make the necessary adjustments to incorporate source terms into the scheme. We proceed in Section 3 with the discretization of the cell-averages of the source terms for the shallow-water equations. The goal is to find a discretization such that the scheme will preserve stationary steady states,

i.e. zero velocities and a flat surface. We show that on general unstructured meshes, there is no discretization of the source terms in the shallow water equations that provide a well-balanced form of the KP scheme. We then proceed by showing how to modify the original scheme in such a way that it is possible to obtain a well-balanced discretization of the source terms. We conclude in Section 4 with numerical examples that demonstrate the accuracy of our scheme as well as its well-balanced property.

2 Central Schemes for Balance Laws on Unstructured Grids

We consider the two-dimensional balance law,

$$u_t + f(u)_x + g(u)_y = S(u, x, y, t), \tag{2.1}$$

subject to the initial data, $u(x, y, 0) = u_0(x, y)$. We are interested in approximating solutions of (2.1) that are computed in terms of cell averages on a fixed unstructured conformal grid. To simplify this exposition we first consider the scalar case. The scheme that is described below can be easily extended component-wise to systems of balance laws. We will make this obvious extension later on when dealing with the specific problem of the system of shallow water equations (1.1).

We focus our attention on the central scheme on triangular meshes that was recently derived in [14]. We briefly overview the derivation of this scheme in the setup of conservation laws of the form

$$u_t + f(u)_x + g(u)_y = 0. \tag{2.2}$$

We assume a conformal triangulation of the domain consisting of cells T_j of area $|T_j|$. The neighboring cells to T_j are denoted by T_{jk}, $k = 1, 2, 3$, while the edge that is joint between T_j and T_{jk} is denoted by E_{jk} and is assumed to be of length h_{jk}. We also denote the outward unit normal to T_j on the k-th edge as n_{jk}, and denote the midpoint of E_{jk} as M_{jk} (see Fig. 2.1).

We assume that the cell averages on all the cells $\{T_j\}$ are known at time t^n,

$$\bar{u}_j^n \approx \frac{1}{|T_j|} \int_{T_j} u(\vec{x}, t^n) d\vec{x}, \tag{2.3}$$

and reconstruct a piecewise-polynomial

$$\tilde{u}^n(x, y) = \sum_j u_j^n(x, y) \chi_j(x, y). \tag{2.4}$$

Here $u_j^n(x, y)$ is a two-dimensional polynomial that is yet to be determined and $\chi_j(x, y)$ is the characteristic function of the cell T_j. To simplify the notations we omit the time-dependence in $u_j(x, y)$. We also denote by $u_{jk}(x, y)$ the polynomial that is reconstructed in the cell T_{jk}.
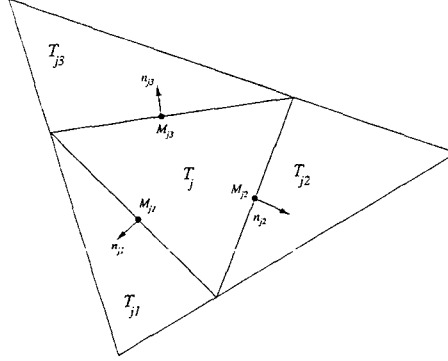
Figure 2.1: The triangular grid

Discontinuities in the interpolant u_j along the edges of T_j propagate with a maximal inward velocity a_{jk}^{in} and a maximal outward velocity a_{jk}^{out}. These velocities can be estimated (for convex fluxes) as

$$
\begin{aligned}
a_{jk}^{\text{in}}(M_{jk}) &= -\min\{\lambda_1[J(u_j(M_{jk})) \cdot n_{jk}], \lambda_1[J(u_{jk}(M_{jk})) \cdot n_{jk}], 0\}, \\
a_{jk}^{\text{out}}(M_{jk}) &= \max\{\lambda_N[J(u_j(M_{jk})) \cdot n_{jk}], \lambda_N[J(u_{jk}(M_{jk})) \cdot n_{jk}], 0\},
\end{aligned}
\tag{2.5}
$$

where $J(u_j(M_{jk}))$ is the Jacobian of the flux $F = (f, g)$ evaluated at M_{jk} and $\lambda_1 < \ldots < \lambda_N$ are its N eigenvalues. These local speeds of propagation are then used to determine evolution points that are away from the propagating discontinuities. An exact evolution of the reconstruction at these evolution points is followed by an intermediate piecewise polynomial reconstruction and finally projected back onto the original cells, providing the cell-averages at the next time-step $\bar{u}_j^{n+1}$. Further details can be found in [14].

A semi-discrete scheme is then obtained at the limit

$$
\frac{d}{dt}\bar{u}_j^n = \lim_{\Delta t \to 0} \frac{\bar{u}_j^{n+1} - \bar{u}_j^n}{\Delta t}.
\tag{2.6}
$$

Most of the terms on the RHS of (2.6) vanish in the limit as $\Delta t \to 0$. The only quantity that has to be determined is a quadrature rule for the integrals of the flux functions over the edges of the cells. If we assume a Gaussian quadrature with m nodes

$$
\int_0^1 \varphi(x)dx \approx \sum_{s=1}^m c_s \varphi(x_s),
$$

which is scaled to h_{jk}, and denote the quadrature points on E_{jk} as G_{jk}^s, the KP scheme for triangular meshes is

$$
\begin{aligned}
\frac{d\bar{u}_j}{dt} &= -\frac{1}{|T_j|} \sum_{k=1}^3 \frac{h_{jk}}{a_{jk}^{\text{in}} + a_{jk}^{\text{out}}} \sum_{s=1}^m c_s \left[\left(a_{jk}^{\text{in}} F(u_{jk}(G_{jk}^s)) + a_{jk}^{\text{out}} F(u_j(G_{jk}^s)) \right) \cdot n_{jk} \right. \\
&\quad \left. - a_{jk}^{\text{in}} a_{jk}^{\text{out}} \left(u_{jk}(G_{jk}^s) - u_j(G_{jk}^s)\right) \right],
\end{aligned}
\tag{2.7}
$$

where $F = (f, g)$. If the fluxes are integrated with a midpoint quadrature (as suggested in [14]) and we use the notation $u_{jk}^{\text{out}} := u_{jk}(M_{jk})$, $u_{jk}^{\text{in}} := u_j(M_{jk})$, $F_{jk}^{\text{in}} := F(u_{jk}^{\text{in}})$, and $F_{jk}^{\text{out}} := F(u_{jk}^{\text{out}})$, the semi-discrete scheme (2.7) becomes

$$\frac{d\bar{u}_j}{dt} = -\frac{1}{|T_j|} \sum_{k=1}^{3} \frac{h_{jk}}{a_{jk}^{\text{in}} + a_{jk}^{\text{out}}} \left[\left(a_{jk}^{\text{in}} F_{jk}^{\text{out}} + a_{jk}^{\text{out}} F_{jk}^{\text{in}} \right) \cdot n_{jk} - a_{jk}^{\text{in}} a_{jk}^{\text{out}} \left(u_{jk}^{\text{out}} - u_{jk}^{\text{in}} \right) \right]. \tag{2.8}$$

A basic observation that will be used below is that the semi-discrete scheme (2.8) is valid for any conformal grid, not necessarily triangular. All that one has to do is to make the suitable adjustments in the notations (e.g. $|T_j|$ being the area of the cell T_j regardless of the shape of that cell) and replace the sum over the three edges of the triangle by a sum over the N_j edges of each cell T_j. When approximating solutions to balance laws of the form (2.1) the scheme has one additional term due to the source term $S(u, x, y, t)$, i.e.

$$\frac{d\bar{u}_j}{dt}(t) = -\frac{1}{|T_j|} \sum_{k=1}^{N_j} \frac{h_{jk}}{a_{jk}^{\text{in}} + a_{jk}^{\text{out}}} \left[\left(a_{jk}^{\text{in}} F_{jk}^{\text{out}} + a_{jk}^{\text{out}} F_{jk}^{\text{in}} \right) \cdot n_{jk} - a_{jk}^{\text{in}} a_{jk}^{\text{out}} \left(u_{jk}^{\text{out}} - u_{jk}^{\text{in}} \right) \right] + \bar{S}_j(t). \tag{2.9}$$

Here

$$\bar{S}_j \approx \frac{1}{|T_j|} \int_{T_j} S(u, \vec{x}, t) d\vec{x}, \tag{2.10}$$

is a discretization of the cell-average of the source term that should be obtained with an appropriate quadrature. It is the discretization of (2.10) that serves as the topic for the next section.

3 A Well-Balanced Scheme

In this section we present a scheme for approximating the solution of (1.1) which is balanced via a discretized average of the source terms. In Section 3.1 we show that the KP scheme (2.9) cannot be balanced using a straightforward discretization of the source terms on general conformal unstructured meshes. In Section 3.2 we present a new scheme based on (2.7), which does allow such balance on general conformal triangular meshes.

3.1 Balancing the KP scheme

Our goal now is to look for a discretization of the source term (2.10) such that the scheme (2.9) will preserve stationary steady-state solutions. Hence, we assume zero velocities, $u = v = 0$, and a constant surface, i.e. $w = \text{Const}$.

Since the first equation in (1.1) is homogeneous, we start by considering the second equation. Similar analysis applies to the third equation. We are therefore looking for a discretization of the average of the source term

$$-(w - B)B_x. \tag{3.1}$$

over the cell T_j. The velocities are zero and therefore the only non-zero component of the flux in (1.1) is

$$f = \frac{1}{2}(w - B)^2. \tag{3.2}$$

This means that in order for the scheme (2.9) to preserve stationary steady-state solutions, the average of the source term (3.1) over the cell T_j has to be discretized such that for f given in (3.2),

$$0 = -\frac{1}{|T_j|} \sum_{k=1}^{N_j} \frac{h_{jk}}{a_{jk}^{\text{in}} + a_{jk}^{\text{out}}} \left[\left(a_{jk}^{\text{in}} f_{jk}^{\text{out}} + a_{jk}^{\text{out}} f_{jk}^{\text{in}} \right) n_{jk,x} \right] + \bar{S}_j. \tag{3.3}$$

Here $n_{jk,x}$ is the component of the normal n_{jk} in the x-direction.

The eigenvalues of the Jacobian of the system (1.1) are $u \pm \sqrt{w - B}$ and u, which are $\pm\sqrt{w - B}$ and 0 in the case of zero velocities. If we assume that w is constant and that the point values of B are known, the one-sided velocities satisfy $a_{jk}^{\text{in}} = a_{jk}^{\text{out}}$. Under these assumptions the condition (3.3) can be rewritten as

$$\bar{S}_j = \frac{1}{|T_j|} \sum_{k=1}^{N_j} h_{jk} \left[\left(\frac{f_{jk}^{\text{out}} + f_{jk}^{\text{in}}}{2} \right) n_{jk,x} \right] = \frac{1}{|T_j|} \sum_{k=1}^{N_j} \frac{h_{jk}}{2} \left[(w - B_{jk})^2 n_{jk,x} \right], \tag{3.4}$$

where $B_{jk} = B\left(M_{jk}\right)$.

We now assume a discretization of the cell-average of the source (3.1) of the form

$$\bar{S}_j = -\sum_{k=1}^{N_j} g_{jk}(w - B_{jk})\mathcal{D}, \tag{3.5}$$

where $\mathcal{D} \approx B_x$, and g_{jk} are yet to be determined. To simplify the notations we denote $m_k = h_{jk}n_{jk,x}$. It is easy to check that $\sum_{k=1}^{N_j} m_k = 0$ and hence in order for the representation (3.5) to be consistent with (3.4) we must have

$$\mathcal{D} = -\frac{1}{2|T_j|} \frac{\sum_{k=1}^{N_j} m_k B_{jk}(B_{jk} - 2w)}{\sum_{k=1}^{N_j} g_{jk}(w - B_{jk})}. \tag{3.6}$$

Since $\mathcal{D}$ in (3.6) should not be a function of w we are seeking constants a_k such that

$$\sum_{k=1}^{N} m_k B_k(B_k - 2w) = \left[\sum_{k=1}^{N} g_k(w - B_k) \right] \left[\sum_{k=1}^{N} a_k B_k \right], \tag{3.7}$$

where for simplicity we omit the obvious j-dependence from all the notations. Eq. (3.7) can be rewritten as

$$\begin{cases} -2\sum_{k=1}^{N} m_k B_k = \sum_{k=1}^{N} g_k \sum_{k=1}^{N} a_k B_k; \\ \\ \sum_{k=1}^{N} m_k B_k^2 = -\sum_{k=1}^{N} g_k B_k \sum_{k=1}^{N} a_k B_k. \end{cases} \tag{3.8}$$
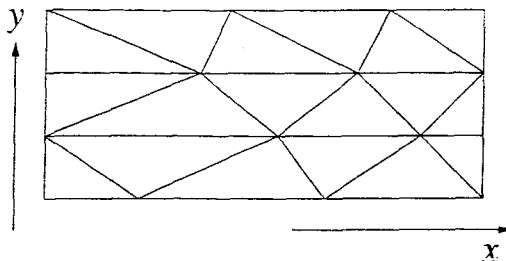
Figure 3.1: An admissible triangular mesh

The coefficients of the powers of B_k in (3.8) produce the following system of equations:

$$
\begin{cases}
-2m_i = a_i \sum_{k=1}^{N} g_k, & i = 1, \dots, N, \\[2mm]
m_i = -a_i g_i, & i = 1, \dots, N, \\[2mm]
a_i g_j = -a_j g_i, & i \neq j, \ i, j = 1, \dots, N.
\end{cases}
\tag{3.9}
$$

Finally, from (3.9) we have

$$
g_i = \frac{1}{2} \sum_{k=1}^{N} g_k, \qquad i = 1, \dots, N.
\tag{3.10}
$$

Eq. (3.10) can generally hold only for $N = 2$, which means that one can expect to be able to balance the scheme (2.9) for stationary steady-state solutions only in cells that have two edges that contribute to the flux in the x-direction. This obviously excludes most meshes. There are two cases of special interest:

1. When the mesh is composed of triangles with one side that is parallel to the x-axis (see Fig. 3.1), each cell has only two edges that contribute to the flux in the x-direction. In this case the system (3.9) can be solved. This result will enable us to introduce in Section 3.2 a modification of the scheme (2.9) that can be balanced on general meshes. Due to symmetry considerations, such a mesh will not satisfy the balance conditions in the y-direction (that come from the third equation in (1.1)) unless all triangles are right triangles that are aligned with both coordinate axes.

2. The scheme can be balanced in both directions in the very special case of Cartesian grids. This corresponds to the case previously solved in [12]. The results of [12] when viewed from the point of view of the system (3.9) amount to the equality

$$
B_1(B_1 - 2w) - B_2(B_2 - 2w) = (2w - B_1 - B_2)(B_2 - B_1).
$$

Remark. If we assume a more general discretization of the cell average of the cell-average of (3.1) of the form

$$
\bar{S}_j = -\sum_{k=1}^{N} g_k(w - B_k) \sum_{k'=1}^{N} a_{kk'} B_{k'},
\tag{3.11}
$$

then the system (3.9) is replaced by (denoting $\tilde{m}_k = m_k/(2|T_j|)$)

$$\begin{cases} -2\tilde{m}_k = \sum_{k'=1}^{N} g_{k'} a_{k'k}, & k = 1, \ldots, N, \\[2mm] \tilde{m}_k = -g_k a_{kk}, & k = 1, \ldots, N, \\[2mm] g_k a_{kk'} = -g_{k'} a_{k'k}, & k \neq k', \; k, k' = 1, \ldots, N. \end{cases} \tag{3.12}$$

Eq. (3.12) can be solved in the general case (unlike Eq. (3.9)). For example, in the case of a triangular grid ($N = 3$) one possible solution (assuming $\tilde{m}_1 \neq 0$ and $\tilde{m}_3 + 2\tilde{m}_2 \neq 0$) is

$$g = \begin{pmatrix} -\tilde{m}_1 \\ \tilde{m}_2 + \frac{\tilde{m}_3}{2} \\ \frac{\tilde{m}_3}{2} \end{pmatrix}, \qquad a = \begin{pmatrix} 1 & \frac{\tilde{m}_3 + 2\tilde{m}_2}{2\tilde{m}_1} & \frac{\tilde{m}_3}{2\tilde{m}_1} \\ 1 & -\frac{2\tilde{m}_2}{2\tilde{m}_2 + \tilde{m}_3} & -\frac{\tilde{m}_3}{2\tilde{m}_2 + \tilde{m}_3} \\ 1 & 1 & -2 \end{pmatrix}. \tag{3.13}$$

If $\tilde{m}_1 = 0$ the expression (3.13) can be replaced, e.g., by

$$g = \begin{pmatrix} 0 \\ \tilde{m}_2 + \frac{\tilde{m}_3}{2} \\ \frac{\tilde{m}_3}{2} \end{pmatrix}, \qquad a = \begin{pmatrix} 0 & \frac{\tilde{m}_3 + 2\tilde{m}_2}{\tilde{m}_3} & 1 \\ 1 & -\frac{2\tilde{m}_2}{2\tilde{m}_2 + \tilde{m}_3} & -\frac{\tilde{m}_3}{2\tilde{m}_2 + \tilde{m}_3} \\ 1 & 1 & -2 \end{pmatrix}. \tag{3.14}$$

If $\tilde{m}_3 + 2\tilde{m}_2 = 0$ a permutation of the numbering of the sides of the triangle will provide a solution. Other solutions of (3.12) exist.

While formally being able to balance the scheme with the expressions (3.13) and (3.14), it remains unclear in what sense $\sum_{k'} a_{kk'} B_{k'}$ approximates the derivative B_x. In other words, it is not obvious that the consistency of this discretization can be established. We therefore consider this approach unsatisfactory.

3.2   A new well-balanced scheme

We focus on conformal triangular grids. Our ideas can be easily extended to other conformal unstructured meshes. In order to create a balanced scheme for (1.1), we propose to decompose every triangle T_j into several triangles as explained below. This requires a different decomposition for the two flux components. For the first component, f, we decompose T_j into two triangles, each of which has an edge parallel to the x-axis. For the second component of the flux we split T_j into two other triangles, each of which has an edge parallel to the y-axis.

We denote the vertices of T_j as V_{jk}, $k = 1, 2, 3$, and define the edges of T_j as $E_{j1} = V_{j2} - V_{j1}$, $E_{j2} = V_{j3} - V_{j2}$ and $E_{j3} = V_{j1} - V_{j3}$. The midpoint of the k-th edge of T_j is M_{jk}. $I(a, b)$ denotes the closed interval with endpoints a and b. We also use $V_{jk,x}$ (or $V_{jk,y}$) to denote the x (or y) component of V_{jk}. To simplify the treatment, we classify the triangles into two categories as portrayed in Fig. 3.2:

- Type 1: one vertex V_{j1} bisects the opposite edge in the y direction: the y-component $V_{j1,y} \in I(V_{j2,y}, V_{j3,y})$ and a different vertex V_{j2} bisects the opposite edge in the x direction: $V_{j2,x} \in I(V_{j1,x}, V_{j3,x})$. (see Fig. 3.2 (left)).

- Type 2: The same vertex V_{j1} bisects the opposite edge in both the x and y direction: $V_{j1,y} \in I(V_{j2,y}, V_{j3,y})$ and $V_{j1,x} \in I(V_{j2,x}, V_{j3,x})$. (see Fig. 3.2 (right)).
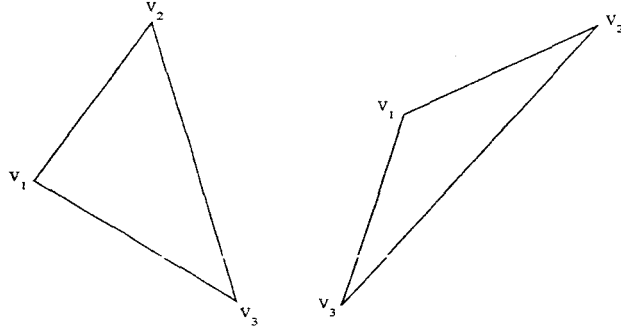
Figure 3.2: The two types of triangles *Left:* Type 1. *Right:* Type 2.
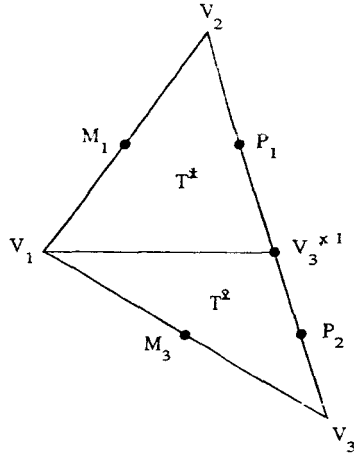
Figure 3.3: The triangle decomposition for the f-flux.

Note that these definitions specify our vertex numbering convention. The decomposition for the g-flux will depend on the type of triangle.

3.2.1 The Decomposition in the x-Direction

For the flux in the x-direction, we decompose T_j into two triangles $T_j^{x,1}$ and $T_j^{x,2}$ (see Fig. 3.3). Define $V_{j3}^{x,1}$ to be the intersection of edge E_{j2} with the line $y = V_{j1,y}$. The vertices of $T_j^{x,1}$ are $V_{j1}^{x,1} := V_{j1}$, $V_{j2}^{x,1} := V_{j2}$, and $V_{j3}^{x,1}$. The vertices of $T_j^{x,2}$ are $V_{j1}^{x,2} := V_{j3}^{x,1}$, $V_{j2}^{x,2} := V_{j3}$, and $V_{j3}^{x,2} := V_{j1}$. For both triangles $T_j^{x,i}$, the lengths of the sides are $h_{jk}^{x,i}$, the corresponding midpoints are $M_{jk}^{x,i}$, the interior and exterior speeds of propagation are $a_{jk}^{in,out,x,i}$ and the normals are $n_{jk}^{x,i} = \left(n_{jk,x}^{x,i}, n_{jk,y}^{x,i}\right)$. These definitions imply $M_{j1}^{x,1} = M_{j1}$, $M_{j2}^{x,2} = M_{j3}$, $h_{j1}^{x,1} = h_{j1}$, $h_{j2}^{x,2} = h_{j3}$, $h_{j2}^{x,1} + h_{j1}^{x,2} = h_{j2}$, $n_{j1}^{x,1} = n_{j1,x}$, $n_{j2}^{x,1} = n_{j1}^{x,2} = n_{j2,x}$, $n_{j1}^{x,2} = n_{j3,x}$, and $n_{j3,x}^{x,1} = n_{j3,x}^{x,2} = 0$. For the velocities we have $a_{j1}^{in,out,x,1} = a_{j1}^{in,out}$, $a_{j2}^{in,out,x,1} = a_{j2}^{in,out}$, $a_{j1}^{in,out,x,2} = a_{j2}^{in,out}$, and $a_{j2}^{in,out,x,2} = a_{j3}^{in,out}$. The velocity $a_{j3}^{in,out,x,i}$ does not play any role in the following computation since $n_{j3,x}^{x,1} = n_{j3,x}^{x,2} = 0$. Finally, the external reconstructions are denoted as $u_{j1}^{x,1} = u_{j1}$, $u_{j2}^{x,1} = u_{j1}^{x,2} = u_{j2}$, and $u_{j2}^{x,2} = u_{j3}$.

On each triangle $T_j^{x,i}$ we denote the cell-average of the component of the flux in the x-direction by Φ_j^i. It is given by

$$\Phi_j^i = -\frac{1}{|T_j^{x,i}|} \sum_{k=1}^{2} \frac{h_{jk}^{x,i} n_{jk,x}^{x,i}}{a_{jk}^{\text{in},x,i} + a_{jk}^{\text{out},x,i}} \left[a_{jk}^{\text{in},x,i} f\left(u_{jk}^{x,i}\left(M_{jk}^{x,i}\right)\right) + a_{jk}^{\text{out},x,i} f\left(u_j\left(M_{jk}^{x,i}\right)\right) \right], \qquad i = 1, 2.$$

The cell-average of the x-component of the flux over the entire cell T_j is taken to be the weighted average

$$\Phi_j := \frac{|T_j^{x,1}|}{|T_j|} \Phi_j^1 + \frac{|T_j^{x,2}|}{|T_j|} \Phi_j^2.$$

Since $\sum_{k=1}^{3} h_{jk} n_{jk} = 0$ we have $h_{j1}^{x,1} n_{j1,x}^{x,1} = -h_{j2}^{x,1} n_{j2,x}^{x,1}$, and $h_{j2}^{x,2} n_{j2,x}^{x,2} = -h_{j1}^{x,2} n_{j1,x}^{x,2}$. Hence, Φ_j can be rewritten as

$$\Phi_j = -\frac{h_{j1} n_{j1,x}}{|T_j|} \left[\frac{a_{j1}^{\text{in}} f_{j1}^{\text{out}} + a_{j1}^{\text{out}} f_{j1}^{\text{in}}}{a_{j1}^{\text{in}} + a_{j1}^{\text{out}}} - \frac{a_{j2}^{\text{in}} f\left(u_{j2}\left(P_{j1}\right)\right) + a_{j2}^{\text{out}} f\left(u_j\left(P_{j1}\right)\right)}{a_{j2}^{\text{in}} + a_{j2}^{\text{out}}} \right] \tag{3.15}$$
$$\qquad -\frac{h_{j3} n_{j3,x}}{|T_j|} \left[\frac{a_{j3}^{\text{in}} f_{j3}^{\text{out}} + a_{j3}^{\text{out}} f_{j3}^{\text{in}}}{a_{j3}^{\text{in}} + a_{j3}^{\text{out}}} - \frac{a_{j2}^{\text{in}} f\left(u_{j2}\left(P_{j2}\right)\right) + a_{j2}^{\text{out}} f\left(u_j\left(P_{j2}\right)\right)}{a_{j2}^{\text{in}} + a_{j2}^{\text{out}}} \right],$$

where $P_{j1} := M_{j2}^{x,1}$ and $P_{j2} := M_{j1}^{x,2}$.

Remark. We would like to note that the flux term (3.15) can be derived directly from (2.7) by changing the quadrature points on E_{j2} to P_1 and P_2.

We now verify that Φ_j given by (3.15) approximates $-f_x$ to second order.

Lemma 3.1 *Assume a smooth reconstruction $\tilde{u}^n(x,y)$ in (2.4). Assume that the flux is linear, i.e., $f(x,y) = ax + by + c$ with constant a and b. Then $\Phi_j = -a$.*

Before proving Lemma 3.1 we consider the following geometrical lemma.

Lemma 3.2 *With M and P defined as above (suppressing j),*

$$M_{1,x} - P_{1,x} = -\frac{|T|}{h_2 n_{2,x}}, \quad M_{3,x} - P_{2,x} = -\frac{|T|}{h_2 n_{2,x}}.$$

Proof. $M_1 = \frac{1}{2}\left(V_1 + V_2\right)$, and for some s, $P_1 = V_2 + s\left(V_3 - V_2\right)$. We require that $P_{1,y} = M_{1,y}$, which implies that

$$s = \frac{1}{2} \frac{V_{1,y} - V_{2,y}}{V_{3,y} - V_{2,y}}.$$

Therefore

$$M_{1,x} - P_{1,x} = \frac{1}{2}\left(V_{1,x} + V_{2,x}\right) - V_{2,x} - \frac{1}{2}\frac{V_{1,y} - V_{2,y}}{V_{3,y} - V_{2,y}}\left(V_{3,x} - V_{2,x}\right) = -\frac{1}{2}\frac{E_1 \times E_2}{E_{2,y}}.$$

When the orientation of the vertices of T_j is clockwise, $E_1 \times E_2 = -2\,|T|$ and $n_2 = \frac{1}{h_2}\left(-E_{2,y}, E_{2,x}\right)$ while when the orientation is counter-clockwise $E_1 \times E_2 = 2\,|T|$ and $n_2 = \frac{1}{h_2}\left(E_{2,y}, -E_{2,x}\right)$, so

$$M_{1,x} - P_{1,x} = -\frac{|T|}{h_2 n_{2,x}}.$$

Similar arguments hold for $M_{3,x} - P_{2,x}$.

Proof. (of Lemma 3.1) Since the reconstruction (2.4) was assumed to be smooth, we have $u_{jk}^{\text{in}} = u_{jk}^{\text{out}}$ and therefore $a_{jk}^{\text{in}} = a_{jk}^{\text{out}}$. In this case

$$\Phi_j = -\frac{h_1 n_{1,x}}{|T|}\left[f(M_1) - f(P_1)\right] - \frac{h_3 n_{3,x}}{|T|}\left[f(M_3) - f(P_2)\right],$$

where we use the notation $f(P) = f(u_j(P))$. For the linear flux $f(x,y) = ax + by + c$ we have

$$
\begin{aligned}
\Phi_j &= -\frac{h_1 n_{1,x}}{|T|}\left[aM_{1,x} + bM_{1,y} - (aP_{1,x} + bP_{1,y})\right] - \frac{h_3 n_{3,x}}{|T|}\left[aM_{3,x} + bM_{3,y} - (aP_{2,x} + bP_{2,y})\right] \\
&= -\frac{h_1 n_{1,x}}{|T|}a\left(M_{1,x} - P_{1,x}\right) - \frac{h_3 n_{3,x}}{|T|}a\left(M_{3,x} - P_{2,x}\right) \\
&= -\frac{h_1 n_{1,x}}{|T|}\left[a\left(-\frac{|T|}{h_2 n_{2,x}}\right)\right] - \frac{h_3 n_{3,x}}{|T|}\left[a\left(-\frac{|T|}{h_2 n_{2,x}}\right)\right] = -a.
\end{aligned}
$$

The second equality holds since $M_{1,y} = P_{1,y}$ and $M_{3,y} = P_{2,y}$, while the third-equality is due to Lemma 3.2 and $\sum_{k=1}^{3} h_{jk} n_{jk} = 0$.

3.2.2 The Decomposition in the y-Direction

Type 1 triangles. We decompose T_j into two triangles $T_j^{y,1}$ and $T_j^{y,2}$ (see Fig. 3.4 (left)). The intersection of the edge E_{j3} with the line $x = V_{j2,x}$ is denoted by $V_{j1}^{y,1}$. The vertices of $T_j^{y,1}$ are $V_{j1}^{y,1}$, $V_{j2}^{y,1} := V_{j1}$, and $V_{j3}^{y,1} := V_{j2}$. The vertices of $T_j^{y,2}$ are vertices $V_{j1}^{y,2} := V_{j2}$, $V_{j2}^{y,2} := V_{j3}$, and $V_{j3}^{y,2} := V_{j1}^{y,1}$. As before, we have $M_{j2}^{y,1} = M_{j1}$, $M_{j1}^{y,2} = M_{j2}$, $h_{j2}^{y,1} = h_{j1}$, $h_{j1}^{y,2} = h_{j2}$, $h_{j1}^{y,1} + h_{j2}^{y,2} = h_{j3}$. The normals $n_{j2}^{y,1} = n_{j1}$, $n_{j1}^{y,1} = n_{j2}^{y,2} = n_{j3}$, $n_{j2}^{y,2} = n_{j2}$, $n_{j3,y}^{y,1} = n_{j3,y}^{y,2} = 0$, and the velocities $a_{j1}^{\text{in,out},y,1} = a_{j3}^{\text{in,out}}$, $a_{j2}^{\text{in,out},y,1} = a_{j1}^{\text{in,out}}$, $a_{j1}^{\text{in,out},y,2} = a_{j2}^{\text{in,out}}$, $a_{j2}^{\text{in,out},y,2} = a_{j3}^{\text{in,out}}$. The velocity $a_{j3}^{\text{in,out},y,i}$ does not appear in the result because $n_{j3,y}^{y,1} = n_{j3,y}^{y,2} = 0$. Finally, the external reconstructions are $u_{j1}^{y,1} = u_{j3}$, $u_{j2}^{y,1} = u_{j1}$, $u_{j1}^{y,2} = u_{j2}$, and $u_{j2}^{y,2} = u_{j3}$.

We denote the cell-averages of the component of the flux in the y-direction on each triangle $T_j^{y,i}$ by Γ_j^i. It is given by

$$\Gamma_j^i := -\frac{1}{|T_j^{y,i}|}\sum_{k=1}^{2}\frac{h_{jk}^{y,i} n_{jk,y}^{y,i}}{a_{jk}^{\text{in},y,i} + a_{jk}^{\text{out},y,i}}\left[a_{jk}^{\text{in},y,i}g\left(u_{jk}^{y,i}\left(M_{jk}^{y,i}\right)\right) + a_{jk}^{\text{out},y,i}g\left(u_j\left(M_{jk}^{y,i}\right)\right)\right], \qquad i = 1, 2.$$

The cell-average of the y-component of the flux over the entire cell T_j is then given by the weighted average

$$\Gamma_j := \frac{|T_j^{y,1}|}{|T_j|}\Gamma_j^1 + \frac{|T_j^{y,2}|}{|T_j|}\Gamma_j^2.$$
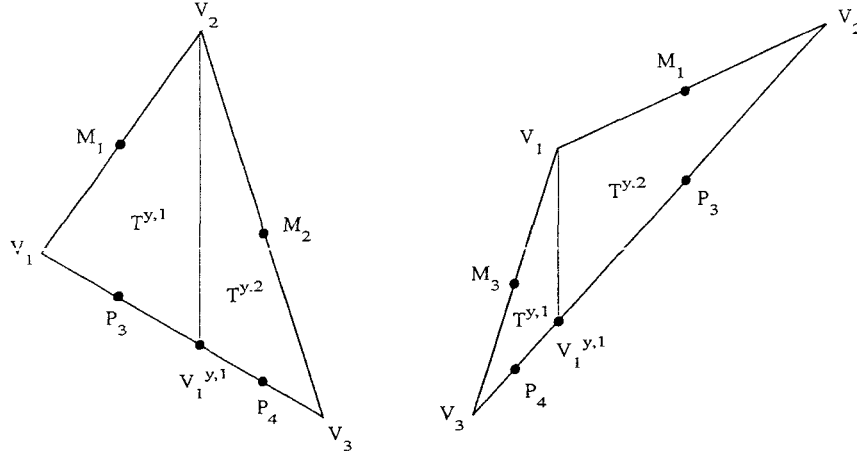
Figure 3.4: The triangle decomposition for the g-flux. *Left:* Type 1. *Right:* Type 2.

Clearly $h_{j2}^{y,1} n_{j2,y}^{y,1} = -h_{j1}^{y,1} n_{j1,y}^{y,1}$, and $h_{j1}^{y,2} n_{j1,y}^{y,2} = -h_{j2}^{y,2} n_{j2,y}^{y,2}$. Therefore Γ_j can be rewritten as

$$
\begin{aligned}
\Gamma_j \;=\; & -\frac{h_{j1} n_{j1,y}}{|T_j|} \left[\frac{a_{j1}^{\mathrm{in}} g_{j1}^{\mathrm{out}} + a_{j1}^{\mathrm{out}} g_{j1}^{\mathrm{in}}}{a_{j1}^{\mathrm{in}} + a_{j1}^{\mathrm{out}}} - \frac{a_{j3}^{\mathrm{in}} g\left(u_{j3}\left(P_{j3}\right)\right) + a_{j3}^{\mathrm{out}} g\left(u_j\left(P_{j3}\right)\right)}{a_{j3}^{\mathrm{in}} + a_{j3}^{\mathrm{out}}} \right] \\
& -\frac{h_{j2} n_{j2,y}}{|T_j|} \left[\frac{a_{j2}^{\mathrm{in}} g_{j2}^{\mathrm{out}} + a_{j2}^{\mathrm{out}} g_{j2}^{\mathrm{in}}}{a_{j2}^{\mathrm{in}} + a_{j2}^{\mathrm{out}}} - \frac{a_{j3}^{\mathrm{in}} g\left(u_{j3}\left(P_{j4}\right)\right) + a_{j3}^{\mathrm{out}} g\left(u_j\left(P_{j4}\right)\right)}{a_{j3}^{\mathrm{in}} + a_{j3}^{\mathrm{out}}} \right] ,
\end{aligned}
\tag{3.16}
$$

where $P_{j3} := M_{j1}^{y,1}$ and $P_{j4} := M_{j2}^{y,2}$.

Type 2 triangles. This case corresponds to Fig. 3.4 (right). Analogous computations to those for Type 1 triangles provide the cell-average of the y-component of the flux over the cell T_j, which this time is given by

$$
\begin{aligned}
\Gamma_j = & -\frac{h_{j1} n_{j1,y}}{|T_j|} \left[\frac{a_{j1}^{\mathrm{in}} g_{j1}^{\mathrm{out}} + a_{j1}^{\mathrm{out}} g_{j1}^{\mathrm{in}}}{a_{j1}^{\mathrm{in}} + a_{j1}^{\mathrm{out}}} - \frac{a_{j2}^{\mathrm{in}} g\left(u_{j2}\left(P_{j3}\right)\right) + a_{j2}^{\mathrm{out}} g\left(u_j\left(P_{j3}\right)\right)}{a_{j2}^{\mathrm{in}} + a_{j2}^{\mathrm{out}}} \right] \\
& -\frac{h_{j3} n_{j3,y}}{|T_j|} \left[\frac{a_{j3}^{\mathrm{in}} g_{j3}^{\mathrm{out}} + a_{j3}^{\mathrm{out}} g_{j3}^{\mathrm{in}}}{a_{j3}^{\mathrm{in}} + a_{j3}^{\mathrm{out}}} - \frac{a_{j2}^{\mathrm{in}} g\left(u_{j2}\left(P_{j4}\right)\right) + a_{j2}^{\mathrm{out}} g\left(u_j\left(P_{j4}\right)\right)}{a_{j2}^{\mathrm{in}} + a_{j2}^{\mathrm{out}}} \right] ,
\end{aligned}
\tag{3.17}
$$

where P_{j3} and P_{j4} are given in Fig. 3.4 (right).

3.2.3   The New Method (for conservation laws)

We would now like to combine all the different ingredients that we developed in the previous section into one scheme. The scheme that we write here is still a scheme for approximating solutions of the conservation law (2.2) without the source term. Based on our preliminary analysis of Section 3.1 we know that we will be able to find an admissible discretization of the source terms that will result with a well-balanced scheme. We will treat the source terms in the next section.

We write two versions of the scheme based on the type of triangle. For type 1 triangles, the discretization of the component of the flux in the x-direction, Φ_j is given by (3.15) while the discretization of the component of the flux in the y-direction, Γ_j, is given by (3.16). In this case the scheme takes the form

$$
\begin{aligned}
\frac{d\bar{u}_j}{dt} \;=\; & -\frac{h_{j1}n_{j1,x}}{|T_j|}\left[\frac{a_{j1}^{\text{in}}f_{j1}^{\text{out}}+a_{j1}^{\text{out}}f_{j1}^{\text{in}}}{a_{j1}^{\text{in}}+a_{j1}^{\text{out}}}-\frac{a_{j2}^{\text{in}}f\left(u_{j2}\left(P_{j1}\right)\right)+a_{j2}^{\text{out}}f\left(u_j\left(P_{j1}\right)\right)}{a_{j2}^{\text{in}}+a_{j2}^{\text{out}}}\right] \\
& -\frac{h_{j3}n_{j3,x}}{|T_j|}\left[\frac{a_{j3}^{\text{in}}f_{j3}^{\text{out}}+a_{j3}^{\text{out}}f_{j3}^{\text{in}}}{a_{j3}^{\text{in}}+a_{j3}^{\text{out}}}-\frac{a_{j2}^{\text{in}}f\left(u_{j2}\left(P_{j2}\right)\right)+a_{j2}^{\text{out}}f\left(u_j\left(P_{j2}\right)\right)}{a_{j2}^{\text{in}}+a_{j2}^{\text{out}}}\right] \\
& -\frac{h_{j1}n_{j1,y}}{|T_j|}\left[\frac{a_{j1}^{\text{in}}g_{j1}^{\text{out}}+a_{j1}^{\text{out}}g_{j1}^{\text{in}}}{a_{j1}^{\text{in}}+a_{j1}^{\text{out}}}-\frac{a_{j3}^{\text{in}}g\left(u_{j3}\left(P_{j3}\right)\right)+a_{j3}^{\text{out}}g\left(u_j\left(P_{j3}\right)\right)}{a_{j3}^{\text{in}}+a_{j3}^{\text{out}}}\right] \\
& -\frac{h_{j2}n_{j2,y}}{|T_j|}\left[\frac{a_{j2}^{\text{in}}g_{j2}^{\text{out}}+a_{j2}^{\text{out}}g_{j2}^{\text{in}}}{a_{j2}^{\text{in}}+a_{j2}^{\text{out}}}-\frac{a_{j3}^{\text{in}}g\left(u_{j3}\left(P_{j4}\right)\right)+a_{j3}^{\text{in}}g\left(u_j\left(P_{j4}\right)\right)}{a_{j3}^{\text{in}}+a_{j3}^{\text{out}}}\right] \\
& +\frac{1}{|T_j|}\sum_{k=1}^{3}h_{jk}\frac{a_{jk}^{\text{in}}a_{jk}^{\text{out}}}{a_{jk}^{\text{in}}+a_{jk}^{\text{out}}}\left[u_{jk}^{\text{out}}-u_{jk}^{\text{in}}\right].
\end{aligned}
\tag{3.18}
$$

Here $P_1 = V_2 - \frac{1}{2}\frac{E_{1,y}}{E_{2,y}}E_2$, $P_2 = V_3 + \frac{1}{2}\frac{E_{3,y}}{E_{2,y}}E_2$, $P_3 = V_1 + \frac{1}{2}\frac{E_{1,x}}{E_{3,x}}E_3$, and $P_4 = V_3 - \frac{1}{2}\frac{E_{2,x}}{E_{3,x}}E_3$.

For type 2 triangles we replace the discretization of Γ_j by the one given in (3.17) ending with

$$
\begin{aligned}
\frac{d\bar{u}_j}{dt} \;=\; & -\frac{h_{j1}n_{j1,x}}{|T_j|}\left[\frac{a_{j1}^{\text{in}}f_{j1}^{\text{out}}+a_{j1}^{\text{out}}f_{j1}^{\text{in}}}{a_{j1}^{\text{in}}+a_{j1}^{\text{out}}}-\frac{a_{j2}^{\text{in}}f\left(u_{j2}\left(P_{j1}\right)\right)+a_{j2}^{\text{out}}f\left(u_j\left(P_{j1}\right)\right)}{a_{j2}^{\text{in}}+a_{j2}^{\text{out}}}\right] \\
& -\frac{h_{j3}n_{j3,x}}{|T_j|}\left[\frac{a_{j3}^{\text{in}}f_{j3}^{\text{out}}+a_{j3}^{\text{out}}f_{j3}^{\text{in}}}{a_{j3}^{\text{in}}+a_{j3}^{\text{out}}}-\frac{a_{j2}^{\text{in}}f\left(u_{j2}\left(P_{j2}\right)\right)+a_{j2}^{\text{out}}f\left(u_j\left(P_{j2}\right)\right)}{a_{j2}^{\text{in}}+a_{j2}^{\text{out}}}\right] \\
& -\frac{h_{j1}n_{j1,y}}{|T_j|}\left[\frac{a_{j1}^{\text{in}}g_{j1}^{\text{out}}+a_{j1}^{\text{out}}g_{j1}^{\text{in}}}{a_{j1}^{\text{in}}+a_{j1}^{\text{out}}}-\frac{a_{j2}^{\text{in}}g\left(u_{j2}\left(P_{j3}\right)\right)+a_{j2}^{\text{out}}g\left(u_j\left(P_{j3}\right)\right)}{a_{j2}^{\text{in}}+a_{j2}^{\text{out}}}\right] \\
& -\frac{h_{j3}n_{j3,y}}{|T_j|}\left[\frac{a_{j2}^{\text{in}}g_{j3}^{\text{out}}+a_{j2}^{\text{out}}g_{j3}^{\text{in}}}{a_{j3}^{\text{in}}+a_{j3}^{\text{out}}}-\frac{a_{j2}^{\text{in}}g\left(u_{j2}\left(P_{j4}\right)\right)+a_{j2}^{\text{in}}g\left(u_j\left(P_{j4}\right)\right)}{a_{j2}^{\text{in}}+a_{j2}^{\text{out}}}\right] \\
& +\frac{1}{|T_j|}\sum_{k=1}^{3}h_{jk}\frac{a_{jk}^{\text{in}}a_{jk}^{\text{out}}}{a_{jk}^{\text{in}}+a_{jk}^{\text{out}}}\left[u_{jk}^{\text{out}}-u_{jk}^{\text{in}}\right].
\end{aligned}
\tag{3.19}
$$

In this case $P_1 = V_2 - \frac{1}{2}\frac{E_{1,y}}{E_{2,y}}E_2$, $P_2 = V_3 + \frac{1}{2}\frac{E_{3,y}}{E_{2,y}}E_2$, $P_3 = V_2 - \frac{1}{2}\frac{E_{1,x}}{E_{2,x}}E_2$, and $P_4 = V_3 + \frac{1}{2}\frac{E_{3,x}}{E_{2,x}}E_2$.

Remark. A simple case of interest is that of coordinate-aligned right triangles. Such triangles can be considered to be of type 1 with $n_{j2,y} = n_{j3,x} = 0$ and $P_{j1} = M_{j2}$ and $P_{j3} = M_{j3}$, which means that the method becomes (taking into account that $\sum_{k=1}^{3} h_{jk}n_{jk} = 0$)

$$
\begin{aligned}
\frac{d\bar{u}_j}{dt} \;=\; & -\frac{1}{|T_j|}\left[\frac{a_{j1}^{\text{in}}f_{j1}^{\text{out}}+a_{j1}^{\text{out}}f_{j1}^{\text{in}}}{a_{j1}^{\text{in}}+a_{j1}^{\text{out}}}h_{j1}n_{j1,x}+\frac{a_{j2}^{\text{in}}f_{j2}^{\text{out}}+a_{j2}^{\text{out}}f_{j1}^{\text{in}}}{a_{j2}^{\text{in}}+a_{j2}^{\text{out}}}h_{j2}n_{j2,x}\right] \\
& -\frac{1}{|T_j|}\left[\frac{a_{j1}^{\text{in}}g_{j1}^{\text{out}}+a_{j1}^{\text{out}}g_{j1}^{\text{in}}}{a_{j1}^{\text{in}}+a_{j1}^{\text{out}}}h_{j1}n_{j1,y}+\frac{a_{j3}^{\text{in}}g_{j3}^{\text{out}}+a_{j3}^{\text{out}}g_{j1}^{\text{in}}}{a_{j3}^{\text{in}}+a_{j3}^{\text{out}}}h_{j3}n_{j3,y}\right] \\
& +\frac{1}{|T_j|}\sum_{k=1}^{3}h_{jk}\frac{a_{jk}^{\text{in}}a_{jk}^{\text{out}}}{a_{jk}^{\text{in}}+a_{jk}^{\text{out}}}\left[u_{jk}^{\text{out}}-u_{jk}^{\text{in}}\right].
\end{aligned}
\tag{3.20}
$$

As expected, in this case the method (3.20) coincides with the KP method (2.8).

3.2.4   Adding the Source Term

We return to the shallow water equations (1.1). Our goal is now to find an admissible discretization of the cell-average of the source terms that will preserve stationary steady states. Such a term will be added to the RHS of (3.18) or (3.19) depending on the type of the triangle. In the following we assume Type 1 triangles. Similar analysis holds for Type 2 triangles. We also note that the first equation in the system (1.1) is homogeneous. This means that we only have to consider the remaining two equations when dealing with the source terms. We recall from Section 3.1 that in stationary steady states all the velocities are equal, $a_{jk}^{\text{in}} = a_{jk}^{\text{out}} = a_{jk}$. Our new method (3.18) for the last two equations of (1.1) then becomes

$$
\begin{aligned}
0 = {} & -\frac{h_{j1}n_{j1,x}}{2\,|T_j|} \left[\begin{pmatrix} (w\,(M_{j1}) - B\,(M_{j1}))^2 \\ 0 \end{pmatrix} - \begin{pmatrix} (w\,(P_{j1}) - B\,(P_{j1}))^2 \\ 0 \end{pmatrix} \right] \\
& -\frac{h_{j3}n_{j3,x}}{2\,|T_j|} \left[\begin{pmatrix} (w\,(M_{j3}) - B\,(M_{j3}))^2 \\ 0 \end{pmatrix} - \begin{pmatrix} (w\,(P_{j2}) - B\,(P_{j2}))^2 \\ 0 \end{pmatrix} \right] \\
& -\frac{h_{j1}n_{j1,y}}{2\,|T_j|} \left[\begin{pmatrix} 0 \\ (w\,(M_{j1}) - B\,(M_{j1}))^2 \end{pmatrix} - \begin{pmatrix} 0 \\ (w\,(P_{j3}) - B\,(P_{j3}))^2 \end{pmatrix} \right] \\
& -\frac{h_{j2}n_{j2,y}}{2\,|T_j|} \left[\begin{pmatrix} 0 \\ (w\,(M_{j2}) - B\,(M_{j2}))^2 \end{pmatrix} - \begin{pmatrix} 0 \\ (w\,(P_{j4}) - B\,(P_{j4}))^2 \end{pmatrix} \right] + \begin{pmatrix} \bar{S}_j^1 \\ \bar{S}_j^2 \end{pmatrix}.
\end{aligned} \tag{3.21}
$$

The last term in (3.21) represents the average of the source, i.e., $\bar{S}_j^1 = \text{avg}(-(w - B)B_x)$ and $\bar{S}_j^2 = \text{avg}(-(w - B)B_y)$, where both averages are taken over T_j.

We use (3.21) to determine the admissible discretizations of the cell-averages of the source terms. For constant w the source terms (given by (3.21)) can be rewritten as

$$
\begin{aligned}
\bar{S}_j^1 = {} & -\frac{h_{j1}n_{j1,x}}{2\,|T_j|}[w_{M_{j1}} - B_{M_{j1}} + w_{P_{j1}} - B_{P_{j1}}][B_{M_{j1}} - B_{P_{j1}}] \\
& -\frac{h_{j3}n_{j3,x}}{2\,|T_j|}[w_{M_{j3}} - B_{M_{j3}} + w_{P_{j2}} - B_{P_{j2}}][B_{M_{j3}} - B_{P_{j2}}], \\
\bar{S}_j^2 = {} & -\frac{h_{j1}n_{j1,y}}{2\,|T_j|}[w_{M_{j1}} - B_{M_{j1}} + w_{P_{j3}} - B_{P_{j3}}][B_{M_{j1}} - B_{P_{j3}}] \\
& -\frac{h_{j2}n_{j2,y}}{2\,|T_j|}[w_{M_{j2}} - B_{M_{j2}} + w_{P_{j4}} - B_{P_{j4}}][B_{M_{j2}} - B_{P_{j4}}].
\end{aligned} \tag{3.22}
$$

Here, we use the notation $w_{M_1} := w\,(M_{j1})$, etc. We take the expressions in (3.22) as the discretization of the source even when w is not constant. Similar expressions can be easily written for Type 2 triangles.

Lemma 3.3 *The source discretizations $\bar{S}_j^i$ given by (3.22) are consistent approximations of the source terms in (1.1), and lead to detailed balance in the stationary steady-state case (3.21).*

Proof. We show that $\bar{S}_j^1 \approx \text{avg}(-(w - B)B_x)$. To simplify the notations we suppress the index j. From Lemma 3.2 we know that $M_{1,x} - P_{1,x} = -\frac{|T|}{h_2 n_{2,x}}$. Since $M_{1,y} = P_{1,y}$ we have

$\frac{B_{M_1}-B_{P_1}}{M_{1,x}-P_{1,x}} = B_x + O\left(|M_1 - P_1|^2\right)$ at the midpoint between M_1 and P_1. Hence the first part of $\bar{S}_j^1$ in (3.22) becomes

$$\frac{h_1 n_{1,x}}{2h_2 n_{2,x}} \left(w_{M_1} - B_{M_1} + w_{P_1} - B_{P_1}\right) \frac{B_{M_1} - B_{P_1}}{M_{1,x} - P_{1,x}} \approx \frac{h_1 n_{1,x}}{2h_2 n_{2,x}} \left(w_{M_1} - B_{M_1} + w_{P_1} - B_{P_1}\right) B_x.$$

Applying a similar argument to the second term of $\bar{S}_j^1$ in (3.22) gives

$$\bar{S}_j^1 \approx \frac{1}{2}\left(\frac{h_1 n_{1,x}}{h_2 n_{2,x}}\left(w_{M_1} - B_{M_1} + w_{P_1} - B_{P_1}\right) + \frac{h_3 n_{3,x}}{h_2 n_{2,x}}\left(w_{M_3} - B_{M_3} + w_{P_2} - B_{P_2}\right)\right) B_x. \quad (3.23)$$

Clearly, the coefficient of B_x in (3.23) is a discretization of a weighted average of $-(w - B)$. For example, when $w - B$ is constant we have

$$\bar{S}_j^1 \approx \frac{h_1 n_{1,x} + h_3 n_{3,x}}{h_2 n_{2,x}} (w - B) B_x = -(w - B) B_x.$$

Similar arguments hold for $\bar{S}_j^2$.

4 Numerical Examples

The scheme developed in Section 3.2 did not assume any particular reconstruction. There are several different second-order reconstructions on triangular meshes that are being used in the literature (see [14] and the references therein). We briefly describe the one we used in our simulations.

The starting point is the limited least-squares estimate of the gradients as done in [2]. The first step is to compute a least-squares estimate of the gradient of a field f on the triangle T_j, $\tilde{\nabla}_j f$. We then limit the gradient $\mathcal{D}_j f$ component by component as

$$\mathcal{D}_j f = \mathcal{MM}\left(\tilde{\nabla}_j f, \tilde{\nabla}_{j1} f, \tilde{\nabla}_{j2} f, \tilde{\nabla}_{j3} f\right),$$

where $\tilde{\nabla}_{jk} f$ is the least-squares gradient estimate on T_{jk} and $\mathcal{MM}$ stands for the usual MinMod limiter

$$\mathcal{MM}\left(x_1, x_2, \ldots\right) := \begin{cases} \min_j\{x_j\}, & \text{if } x_j > 0, \forall j, \\ \max_j\{x_j\}, & \text{if } x_j < 0, \forall j, \\ 0, & \text{otherwise.} \end{cases}$$

We use the gradients $\mathcal{D}_j$ to construct a piecewise linear reconstruction for the point-values of each triangle edge E_{jk} as

$$u_j(\vec{x}) = \bar{u}_j + \mathcal{MM}\left(\mathcal{D}_j u \cdot (\vec{x} - \vec{x}_j), \mathcal{D}_{jk} u \cdot (\vec{x} - \vec{x}_j)\right).$$

Here $\mathcal{D}_{jk} u$ is the limited gradient estimate on T_{jk}, $\vec{x}_j$ is the center of T_j and $\vec{x} \in E_{jk}$. We find that this double use of the MinMod limiter minimizes spurious oscillations while preserving the second-order accuracy of the reconstruction.
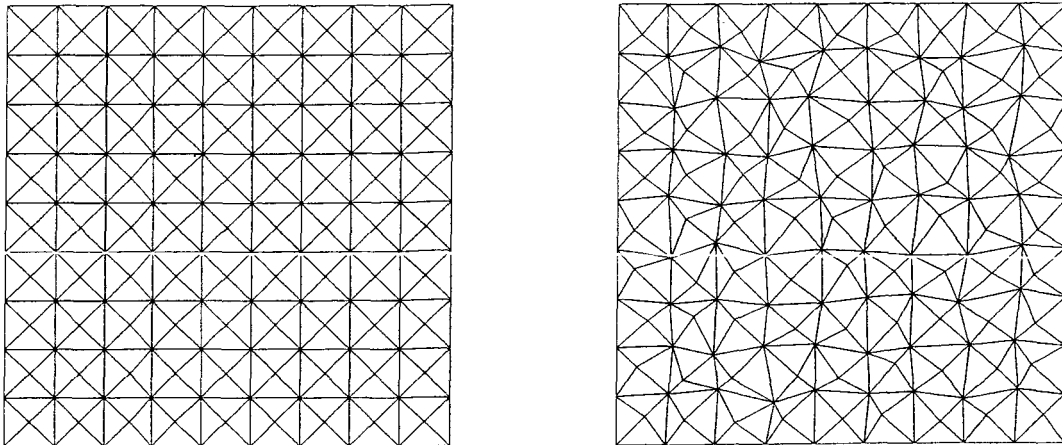
Figure 4.1: The two types of triangle meshes. *Left:* Uniform triangulation. *Right:* Perturbed triangulation.

We use an adaptive time step given by

$$\Delta t = 0.9 \min_{j} \frac{r_j}{|\lambda_N^j|},$$

where r_j is the radius of T_j and $|\lambda_N^j|$ is the norm of the largest eigenvalues of the Jacobian of the flux on T_j.

We use two types of meshes in most of our simulations. The first is a uniform triangulation of a Cartesian mesh with $N \times N$ nodes and constant spacings Δx and Δy, which divides each Cartesian cell into four triangles. To test our method on more general meshes, our second type of mesh is generated from a uniform triangular mesh with a perturbation of the coordinates of the interior vertices. Examples of both meshes are shown in Fig. 4.1. The only exception is Example 6, which uses a uniform triangulation of a warped Cartesian mesh.

Example 1: accuracy tests for a 2D linear advection equation

We test the accuracy of our method (3.18)–(3.19) when applied to the two-dimensional linear advection problem

$$\begin{cases} u_t + u_x + u_y = 0, & (x,y) \in [0,1]^2, \\ u(x, y, t=0) = \sin(2\pi x) + \cos(2\pi y), \end{cases} \tag{4.1}$$

with periodic boundary conditions. The relative L^1-error (i.e. the L^1-error divided by the L^1-norm of the exact solution) at $T = 1$ is shown in Table 4.1 for both uniform and perturbed triangulations, demonstrating the second-order accuracy of our method.

	Uniform Triangulation		Perturbed Triangulation	
N	relative L^1-error	L^1-order	relative L^1-error	L^1-order
10	0.123	–	0.129	–
20	0.029	2.09	0.034	1.94
40	6.52×10^{-3}	2.15	8.68×10^{-3}	1.95
80	1.73×10^{-3}	1.91	3.02×10^{-3}	1.52

Table 4.1: L^1-error and convergence rates for the advection equation (4.1) at $T = 1$ on a uniform and a perturbed triangulation of an $N \times N$ Cartesian mesh.

Example 2: accuracy tests for a 2D Burgers equation

We continue by checking the accuracy of our method (3.18)–(3.19) on non-linear problems by applying it to the two-dimensional Burgers equation

$$\begin{cases} u_t + \frac{1}{2}\left(u^2\right)_x + \frac{1}{2}\left(u^2\right)_y = 0, & [-2\pi, 2\pi]^2, \\ u\left(x, y, t = 0\right) = \sin\left(\frac{x+y}{2}\right), \end{cases} \qquad (4.2)$$

with periodic boundary conditions. The L^1-error of our method at $T = 0.5$ is shown in Table 4.2 for uniform and perturbed triangulations. The computed cell-averages after singularity formation at $T = 1.5$ are shown in Fig. 4.2. Note the sharp shocks that are captured by our method.

	Uniform Triangulation		Perturbed Triangulation	
N	relative L^1-error	L^1-order	relative L^1-error	L^1-order
10	0.064	–	0.064	–
20	0.014	2.20	0.014	2.20
40	4.68×10^{-3}	1.58	4.65×10^{-3}	1.59
80	1.37×10^{-3}	1.77	1.36×10^{-3}	1.77

Table 4.2: L^1-error and convergence rates for Burgers equation (4.2) at $T = 0.5$ on a uniform and a perturbed triangulation of an $N \times N$ Cartesian mesh.

Example 3: accuracy tests for 2D systems

To test our method (3.18)–(3.19) on a system of equations we apply it to the Sod problem for the Euler equations

$$\begin{pmatrix} \rho \\ \rho u \\ \rho v \\ E \end{pmatrix}_t + \begin{pmatrix} \rho u \\ \rho u^2 + p \\ \rho u v \\ u\left(E + p\right) \end{pmatrix}_x + \begin{pmatrix} \rho v \\ \rho u v \\ \rho v^2 + p \\ v\left(E + p\right) \end{pmatrix}_y = 0. \qquad (4.3)$$
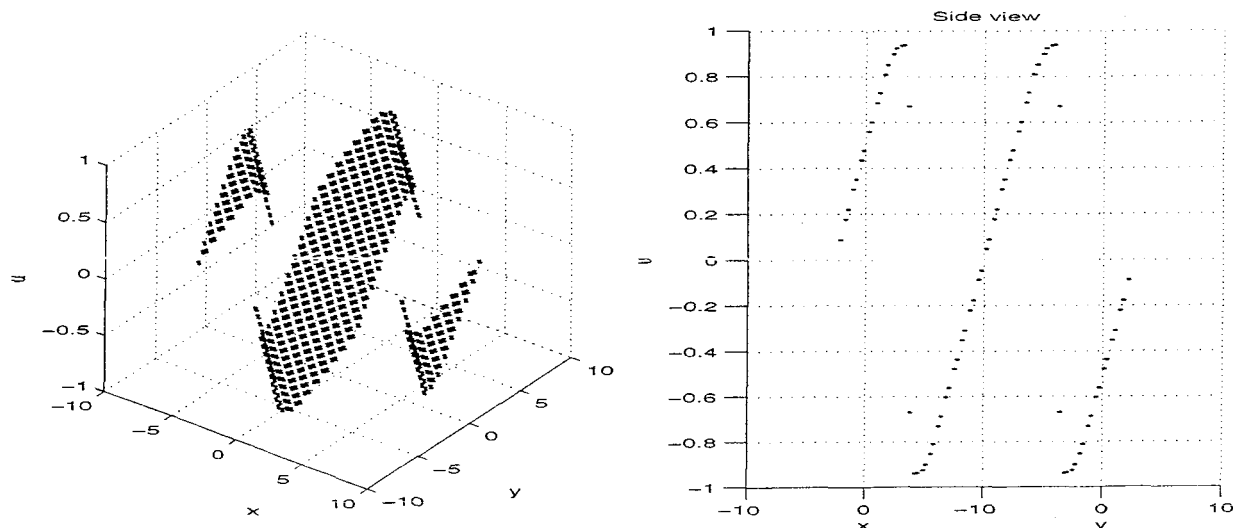
Figure 4.2: Burgers equation at $T = 1.5$ on a uniform triangulation of a 20×20 Cartesian mesh. *Left:* oblique view. *Right:* side view.

Here ρ is the density, (u, v) is the velocity, and E is the energy. The equation of state for the pressure is $p = (\gamma - 1) \left[E - \frac{\rho}{2} (u^2 + v^2) \right]$. We set $\gamma = 1.4$ and take the initial conditions (constant in the y-direction)

$$(p, \rho, u, v) = \begin{cases} (1.0, 1.0, 0.0, 0.0), & x < 0.5, \\ (0.1, 0.125, 0.0, 0.0), & x > 0.5. \end{cases} \tag{4.4}$$

Figure 4.3 shows the computed cell-averages at $T = 0.16$ using our method from Section 3.2 projected onto the $y = 0$ plane. A reference one-dimensional solution is also shown. The two-dimensional problem uses a uniform triangulation based on a 300×30 Cartesian mesh on the domain $[0, 1] \times [0, 0.1]$. The one-dimensional reference solution is computed using the second-order central method of [13] with 3000 points in the domain $[0, 1]$.

Example 4: a balance test

In this example we demonstrate the well-balanced property of our scheme (3.18)–(3.19) with the source discretization (3.22).

As a simple test of balance, we consider the shallow water problem with initial conditions that represent a stationary steady-state. We choose $w(x, y, t = 0) = 2$, $u(x, y, t = 0) = v(x, y, t = 0) = 0$ and a bottom topography given by $B(x, y) = \sin(2\pi x) + \cos(2\pi y)$ on the domain $[0, 1]^2$. We assume periodic boundary conditions. This initial value problem has the trivial stationary steady state solution $w(x, y, t) = 2$, $u(x, y, t) = v(x, y, t) = 0$ for all t.

The relative L^1-errors at $T = 1$ on both uniform and perturbed triangulations based on a 10×10 Cartesian mesh are given in Table 4.3. This table also shows the result found using the KP method [14] with the same source discretization (3.22) which is not balanced for this scheme. We see that our method balances to machine accuracy.
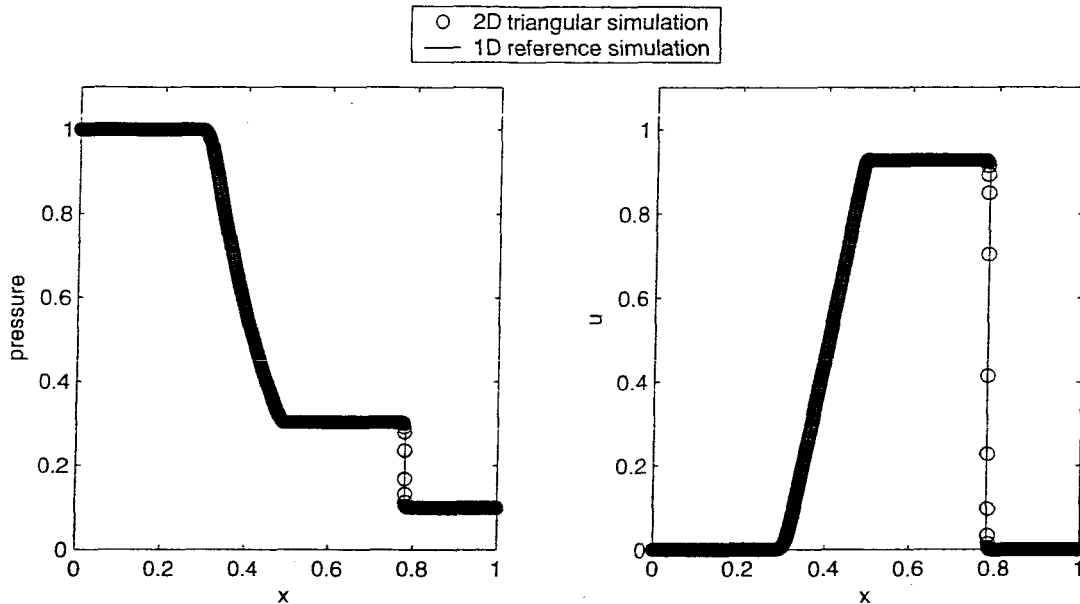
Figure 4.3: The pressure (*left*) and u-velocity (*right*) fields of the Sod problem at $T = 0.16$ on a uniform triangulation. The circles show a projection onto the $y = 0$ plane of the solution of the 2D problem on a triangular mesh. The line shows a 1D reference solution computed with the second-order central-upwind method of [13].

Method	Uniform Triangulation	Perturbed Triangulation
(3.18)–(3.19)–(3.22)	3.5×10^{-17}	6.9×10^{-19}
[14] + (3.22)	3.0×10^{-3}	3.5×10^{-3}

Table 4.3: The relative L^1-error in the balance for (3.18)–(3.19)–(3.22) and for the KP scheme with the source discretization (3.22)

Example 5: propagating waves with a bottom topography

We apply our method to a test problem from [16] of a small perturbation of a steady state problem on the domain $[0, 2] \times [0, 1]$ with periodic boundary conditions in y-direction. The bottom topography is the elliptical Gaussian mound given by

$$B(x, y) = 0.8 \exp\left(-5(x - 0.9)^2 - 50(y - 0.5)^2\right),$$

and the initial conditions are

$$(w, u, v) = \begin{cases} (1.01, 0.0, 0.0), & \text{if } 0.05 < x < 0.15, \\ (1.0, 0.0, 0.0), & \text{otherwise.} \end{cases}$$

Fig. 4.4 shows the result of our method at various times on a uniform triangulation of both a 200×100 and 400×200 Cartesian mesh. These results are in good agreement with other methods on Cartesian grids (see [12, 16]).

Example 6: converging-diverging channel with bottom topography

Our final example is that of a converging-diverging channel with critical flow adapted from [10]. The channel is defined on the domain $[0, 3] \times [-0.5, 0.5]$ with a half-cosine constriction centered at $x = 1.5$. The mesh for this example is shown in Fig. 4.5 (a). It is a uniform triangularization of the warped Cartesian mesh defined by the mapping $(x, y) \rightarrow (x, (1 - 0.2 \cos^2(\pi(x - 1.5))) y)$ when $|x - 1.5| < 0.5$. The initial data is $w = 1, u = v = 0$. The y-boundaries are reflecting. The left x-boundary is an inflow boundary with $u = 5.0$ and the right x-boundary is a zeroth-order outflow boundary. We run the simulations on a 90×30 mesh until $T = 7$ after the steady state is achieved.

We first present this example with a flat bottom, with contours of w shown in Fig. 4.5 (b). Fig. 4.5 (c) shows the same channel at the same time with bottom topography

$$B(x, y) = 0.8\left(\exp\left(-10(x - 1.9)^2 - 50(y - 0.2)^2\right) + \exp\left(-20(x - 2.2)^2 - 50(y + 0.2)^2\right)\right).$$

This topography is shown in Fig. 4.5 (d) and represents two elliptical Gaussian mounds just down-flow from the constriction.

References

[1] Arminjon P., Viallon M.-C., *Généralisation du schéma de Nessyahu-Tadmor pour une équation hyperbolique à deux dimensions d'espace*, C.R. Acad. Sci. Paris, t. **320**, série I. (1995), pp.85–88.

[2] Arminjon P., Viallon M.-C., Madrane, A., *A finite volume extension of the Lax-Friedrichs and Nessyahu-Tadmor schemes for conservation laws on unstructured meshes*, IJCFD Paris, **29** (1997), pp.1-22.

[3] Audusse E., Bristeau M.-O., *Transport of pollutant in shallow water: a two time steps kinetic method*, Math. Model. and Numer. Anal., **37** (2003), pp.389–416.
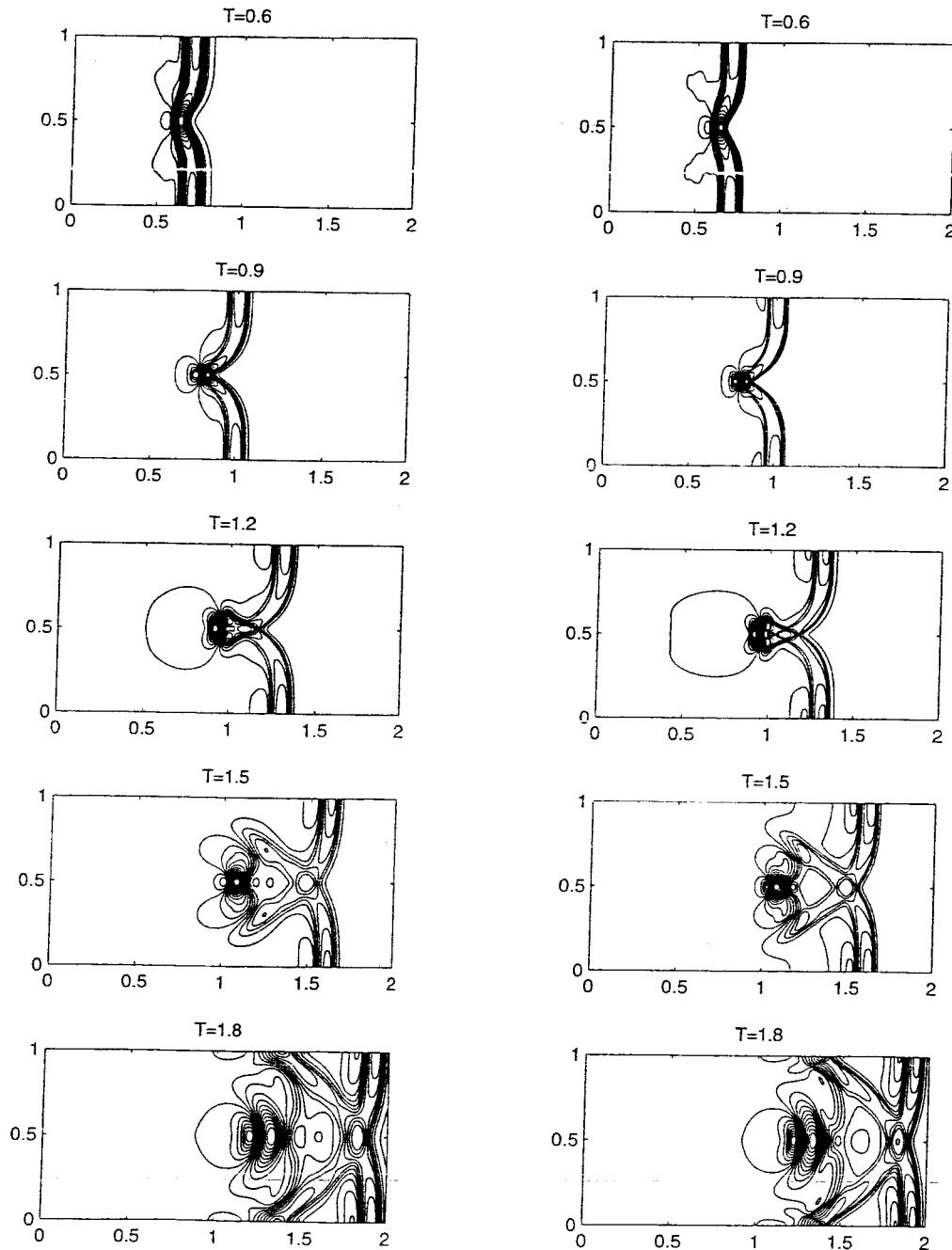
Figure 4.4: Wave propagation over an elliptical hump at various times. *Left:* uniform triangularization based on a 200×100 mesh. *Right:* uniform triangularization based on a 400×200 mesh.
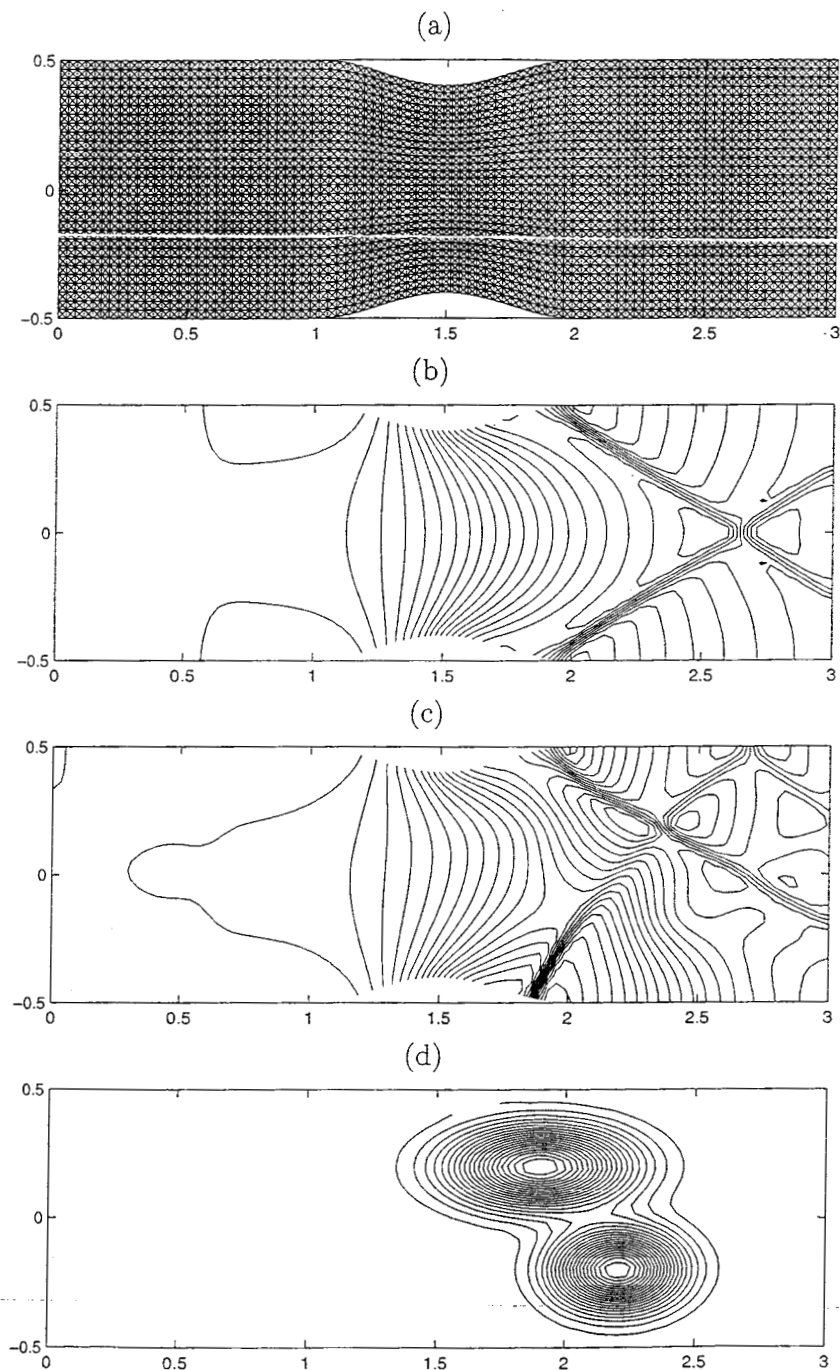
Figure 4.5: Example 6: (a) The mesh. (b) Contours of w for a critical flow through a converging-diverging channel with flat bottom at $T = 7$. (c) Contours of w for a critical flow through a converging-diverging channel with the topography shown below at $T = 7$. (d) The bottom topography for figure (c).

[4] Audusse E., Bristeau M.-O., Perthame B., *Kinetic schemes for Saint-Venant equations with source terms on unstructured grids*, INRIA Report RR-3989, (2000).

[5] Delis A.I., Katsaounis Th., *Relaxation schemes for the shallow water equations*, Int. J. Numer. Meth. Fluids, **41** (2003), pp.695–719.

[6] Friedrichs K. O., Lax P. D., *Systems of Conservation equations with a convex extension*, Proc. Nat. Acad. Sci., **68** (1971), pp.1686–1688.

[7] Gallouët T., Hérard J.-M., Seguin N., *Some approximate Godunov schemes to compute shallow-water equations with topography*, Comput. Fluids., **32** (2003), pp.479–513.

[8] Gerbeau J.F., Perthame B., *Derivation of viscous Saint-Venant system for laminar shallow water; numerical validation*, Discrete Contin. Dyn. Syst. Ser. B, **1** (2001), pp.89–102.

[9] Gosse L., *A well-balanced scheme using non-conservative products designed for hyperbolic systems of conservation laws with source terms*, Math. Models Methods Appl. Sci., **11** (2001), pp.339–365.

[10] Hubbard, M. E., *On the Accuracy of One-Dimensional Models of Steady Converging/Diverging Open Channel Flows*, Int. J. Numer. Meth. Fluids, **35** (2001), pp.785–808.

[11] Jiang G.-S., Tadmor E., *Nonoscillatory central schemes for multidimensional hyperbolic conservation laws*, SIAM J. Sci. Comp., **19** (1998), pp.1892–1917.

[12] Kurganov A., Levy D., *Central-upwind schemes for the Saint-Venant system*, Math. Model. and Numer. Anal., **36** (2002), pp.397–425.

[13] Kurganov A., Noelle S., Petrova G., *Semi-discrete central-upwind schemes for hyperbolic conservation laws and Hamilton-Jacobi equations*, SIAM J. Sci. Comp., **23** (2001), pp.707–740.

[14] Kurganov A., Petrova G., *Central-upwind schemes on unstructured grids for hyperbolic systems of conservation laws*, 2003, submitted.

[15] Kurganov A., Tadmor E., *New high-resolution central schemes for nonlinear conservation laws and convection-diffusion equations*, J. Comput. Phys., **160** (2000), pp.214–282.

[16] LeVeque R.J, *Balancing source terms and flux gradients in high-resolution Godunov methods: the quasi-steady wave-propagation algorithm*, J. Comput. Phys., **146** (1998), pp.346–365.

[17] LeVeque R.J., Bale D.S., *Wave propagation methods for conservation laws with source terms*, Hyperbolic Problems: Theory, Numerics, Applications, Vol. II (Zürich, 1998), pp.609–618, Internat. Ser. Numer. Math., 130, Birkhäuser, Basel, 1999.

[18] Liotta S.F., Romano V., Russo G., *Central schemes for systems of balance laws*, Hyperbolic Problems: Theory, Numerics, Applications, Vol. II (Zürich, 1998), pp.651–660, Internat. Ser. Numer. Math., 130, Birkhäuser, Basel, 1999.

[19] Nessyahu H., Tadmor E., *Non-oscillatory central differencing for hyperbolic conservation laws*, J. Comput. Phys., **87** (1990), pp.408–463.

[20] Perthame B., Simeoni C., *A kinetic scheme for the Saint-Venant system with a source term*, Calcolo, **38** (2001), pp.201–231.

[21] Russo G., *Central schemes for balance laws*, Hyperbolic problems: theory, numerics, applications, Vol. I, II (Magdeburg, 2000), pp.821–829, Internat. Ser. Numer. Math., 140, 141, Birkhäuser, Basel, 2001.

[22] de Saint-Venant A.J.C., *Théorie du mouvement non-permanent des eaux, avec application aux crues des rivière at à l'introduction des marées dans leur lit*, C.R. Acad. Sci. Paris, **73** (1871), pp.147–154.